Isotope-enrichment reveals active viruses follow microbial host dynamics during rewetting of a California grassland soil

Alexa M. Nicolas[1], Ella T. Sieradzki[2], Jennifer Pett-Ridge[3, 4], Jillian F. Banfield[2,5,6], Michiko E. Taga[1], Mary K. Firestone[2,6], Steven J. Blazewicz[3*]

[1]Plant & Microbial Biology Department, University of California, Berkeley, CA, USA
[2]Environmental Science, Policy & Management Department, University of California, Berkeley, CA, USA
[3]Physical and Life Sciences Directorate, Lawrence Livermore National Laboratory, Livermore, CA, USA
[4]University of California Merced, Life & Environmental Sciences Department, Merced, CA, USA
[5]Earth and Planetary Sciences, University of California, Berkeley, CA, USA
[6]Lawrence Berkeley National Laboratory, Berkeley, California, CA, USA
[*]Corresponding author email: blazewicz1@llnl.gov

ABSTRACT

Soil viruses are highly abundant and ubiquitous, yet their impact on soil microbiome structure and function remains essentially unknown. We quantified how viruses and their hosts respond to the first rainfall of the year in seasonally dry soils – a moment commonly referred to as "wet-up", when resident soil microbes are both resuscitated and lysed, with a disproportionately large effect on annual carbon turnover. We applied time-resolved metagenomics, viromics, and quantitative stable isotope probing to track spatiotemporal virus-host trends, and quantify cell death (and by proxy, the amount of biomass carbon released). Dry soil is a sparse yet diverse reservoir of putative virions, of which only a subset thrives following wet-up. A massive degradation of distinct viruses occurs within 24h post wet-up, but after one-week, viral biomass increased by up to seven-fold. Thriving viruses were not induced temperate phages. Our measures of viral-mediated microbial host death indicate that viruses drive a consistent rate of cell lysis after wet-up. These calculations – the first to demonstrate the quantitative impact of viral effects on soil microbiomes and carbon cycling – evidence that viruses significantly impact microbial community assembly. However, viruses do not appear to serve as top-down controls on soil microbial communities following wet-up.

INTRODUCTION

Soil is a highly complex microbial environment and home to tens of millions of unique microbial populations [1], with both biotic and abiotic factors influencing their assembly into complex microbial communities [2–4]. Moments of acute pressure on a community such as rapid environmental changes or fluxes in resource availability drive successional trajectories that result in differing community structures; the first rainfall following the dry season, wet-up, is such a moment [5–9]. However, the role of viruses in soil microbiome structuring remains unknown. Soil viruses are abundant and ubiquitous: a gram of soil can hold more than 10^9 viral-like particles (VLPs) [1, 10]. Recent metagenomic studies of soil viruses have expanded our appreciation of the many functions viruses may perform [11–13], but much remains unknown about how viruses impact soil microbiome turnover and community assembly, especially in response to a perturbation. In this study, we looked to a moment of annual transition in the soil microbiome to establish the role of viruses in soil microbial community assembly.

In arid and semi-arid soils that experience prolonged periods of water-deficit, the first rainfall serves as a pivotal moment which resuscitates activity in the soil microbial community and disproportionately contributes to annual carbon turnover [7, 14]. Immediately following the wet-up of dry soil there is a rapid efflux of mineralized CO_2, termed the "Birch Effect" [15]. Previous

studies suggest this CO_2 pulse is driven by the rapid growth and death of soil microorganisms [7, 16, 17], but the mechanisms of mortality following rewetting are unclear. Microbial mortality after wet-up is not equitably distributed among bacterial phyla – Actinobacteria and Proteobacteria consistently have higher mortality rates [8]. Given the high degree of taxon-specific mortality quantified during wet-up, we hypothesized viruses act as a top-down control in community assembly and drive the differential mortality observed.

In marine systems, viruses are critically important to biogeochemistry, killing upwards of ~40% of bacteria daily and redistributing up to 55% of bacterial carbon in the proposed 'viral shunt' [18–20]. This outsized microbiome impact largely occurs in two additional ways: 1) through targeted predation which influences microbial composition, and 2) via alterations of community function caused by changes in community composition and expression of viral-encoded metabolisms [18, 21–23]. Despite the recent development of soil viromic methods [24, 25], viral contributions to soil organic matter turnover or microbial mortality have yet to be quantified due to the massive diversity of soil microbes, inactivity of many of these microbes, and challenges of preforming microscopy on soil [26].

In arid soil systems, abundant extracellular DNA and dormant cells can occlude distinguishing active microbial cells [27–29], since up to 75% of cells present in soil may be inactive at any given time [30]. Stable isotope probing (SIP) approaches enable the direct identification of active microbes through the tracing of stable isotopes into microbial DNA and other biomolecules [31–33]. Measuring the shift in DNA density following assimilation of a stable isotope, such as ^{18}O via $H_2{}^{18}O$ [34], facilitates the quantification of growth and mortality rates of microbes, termed quantitative stable isotope probing (qSIP) [8, 35, 36]. SIP techniques have proved powerful in identifying active microbes that metabolize soil organic matter and serve crucial roles in nutrient cycling [37, 38], and has been used to identify active soil viral populations and viral-host linkages [38–40].

The rapid growth and death of bacteria following wet-up suggests that wet-up may alter viral activities. Previous studies have characterized the immense taxonomic diversity and functions of soil viruses [41, 42]. Soil DNA viruses encode a variety of metabolisms implicated in nutrient cycling including glycosyl hydrolases, chitin and polysaccharide degradation, ammonia oxidation, and sulfur metabolism [25, 41, 43, 44]. Other work has shown that soil bacteria can maintain lysogenic viral populations in their genomes as prophages [45, 46]. Pure culture research demonstrates these prophages often encode an integrase gene enabling phage recombination into the host chromosome [47, 48]. Prophages, upon certain cues, may excise from host chromosomes entering a lytic cycle, ultimately lysing their host cell. Induction of prophage – the switching from lysogenic to lytic cycle – can occur due to population stochasticity, by an external stress that may cause DNA damage, or through quorum sensing pathways [49, 50]. Temperate phages dominate certain marine systems and switching between lysogenic and lytic cycles corresponds to increased bacterial production [51]. Similarly, integrase-encoding phages have been found at higher abundances in locations associated with more environmental stresses [52]. Given the unique challenges of the soil environment – extraordinary spatial heterogeneity, lack of mixing, microniches of low nutrient availability [53] – some hypothesize that lysogeny may be a predominant lifestyle of soil phages [12, 46, 50, 54–56]. In soil, environmental conditions that drive lysogeny and prophage induction largely remain unknown [45, 57]. Previous studies have shown that soil moisture modulates soil viral counts, composition, and activity [58, 59]. Further, the summer dry-down marks a stretch of time where soil microbes maintain low activity and rates of replication [7, 9, 16, 60] and low host abundance is thought to favor conditions for lysogeny [50, 61, 62]. Thus, we hypothesized that

rewetting of soil serves as an environmental inducer of viruses that had persisted through the summer-dry down as prophages.

Here, we quantified VLPs in soil and released during host infections using a combination of time-resolved viromics and qSIP-informed metagenomics to understand of the role of viruses in restructuring the soil microbiome following wet-up. We address the question of whether rewetting is a major inducer of prophages. The work builds on our previous efforts to link taxon-specific population dynamics with rainfall-induced carbon fluxes [8, 16]. Our analyses quantify contributions of viruses to microbial mortality, thus elucidate the contributions of viruses to the 'Birch Effect'.

MATERIALS AND METHODS

Field sample collection

Topsoil samples (0-15 cm, roughly 0.5 m^3) from replicate field plots were collected from the Hopland Research and Extension Center (HREC) in Northern California, which is unceded land of the Shóqowa and Hopland People, on August 28th, 2018 (only 100% precipitation plots were used for this study, see our paired study Sieradzki et al. 2022 [63] for full detail). During the growing season the same field plots were covered by mixed grassland flora with *Avena sp*. (wild oat) as the most abundant plant. Soil was collected before the first rainfall event of the season and average gravimetric soil moisture was 3%. The dry soil was transferred to Lawrence Livermore National Laboratory (LLNL) where it was homogenized and sieved (2mm) to remove large rocks and roots.

Wet-up experiment

5 g sieved soil from each of 3 field replicates was weighed into separate 15 mL Nalgene flat bottom vials. Soil was wetted to 22% average gravimetric soil moisture with either $H_2{}^{18}O$ (98 at% ^{18}O) or $H_2{}^{16}O$ (natural abundance SIP controls) (Figure 1), after which the vials were sealed inside 500 mL mason jars and incubated at room temperature in the dark. Three incubation treatments were established, each in triplicate: 1) $H_2{}^{16}O$ amended (used for DNA extraction, shotgun sequencing, unfractionated DNA metagenomics and as a fractionated DNA control for qSIP); 2) watered with $H_2{}^{18}O$ for DNA extraction, density centrifugation, shotgun sequencing, and metagenomics (isotopically-labeled fractionated DNA for qSIP); 3) watered with $H_2{}^{16}O$ for viral-like particle (VLP) suspension, concentration, DNAse treatment followed by DNA extraction and shotgun sequencing to generate viromes (unfractionated DNA for viromics). Parallel jars were destructively harvested at 0, 3, 24, 48, 72, and 168 hours following the water addition; at each harvest, soil vials were frozen in liquid nitrogen and then stored at -80 °C.

Viral metagenomes ("viromes")

Soil viromes were generated as described in Nicolas et al. 2021 [64] to assess viruses detected as VLPs i.e. extracellularized. Briefly, two 5-gram soil microcosms from each of three field replicates watered with $H_2{}^{16}O$ were combined for 10 g soil virome extractions. Soil was buffered with a potassium citrate solution and the effluent was passed through a 0.2-µm filter, concentrated, and treated with DNase to remove extracellular DNA. Prior to DNA extraction using a phenol:chloroform strategy, we used an iron flocculation step to concentrate 0.2-µm filtered and concentrated samples as described in Nicolas et al. 2021 [64]. DNA was sequenced on an Illumina Novaseq (2x150 cycles) (UC Davis). Sequencing was performed to attain an average 40 Gb per sample. Illumina adapters and phiX were removed from resulting sequences using BBTools (https://jgi.doe.gov/data-and-tools/bbtools/) and then quality trimmed using Sickle [65]. Sequences were assembled with MEGAHIT version 1.2.9 [66]; we co-assembled all

biological replicates per time point using default parameters. Reading frames were predicted for each contig using Prodigal [67] and were annotated using sequence similarity searches with USEARCH [68] to KEGG [69], uniref [70], and uniport [71].

Metagenome assembled genomes (MAGs) from viromes
To generate microbial bins from the size-fractionated metagenomes, i.e. viromes, we used multiple binning methods. Contigs were binned using Maxbin [72], MetaBAT [73], Concoct [74], and manually based on coverage, GC content, and taxonomy using in house tools on ggkbase (https://ggkbase.berkeley.edu). DASTool [75] was used to predict best bins and bins were further manually curated on ggKbase to remove highly divergent sequences based on coverage, GC, and taxonomy. MAGs from viromes were clustered and dereplicated alongside MAGs from metagenomes (discussed below) using dRep [76] requiring at least 75% completeness and no more than 10% contamination, yielding 39 genomes from candidate phyla radiation bacteria and archaea.

Viral prediction and generation of viral operational taxonomic unit (vOTU) set
To establish a set of viral genomes from our metagenomic efforts we used multiple methods of prediction and dereplicated vOTUs across samples. Viruses were predicted from metagenome and virome contigs. Viruses were predicted using: virsorter1 [77] (all categories), virsorter2 [78] (dsDNA and ssDNA only), VIBRANT [79], deepvirfinder [80] (score ≥ 0.9; pvalue ≤ 0.5), and seeker [81]. From the set of virome and metagenome contigs explored 3,979,792 were predicted to be viral. Of these, 777,725 contigs were designated viral by more than one tool, and 32,660 of this subset were either circularized contigs by VRCA [82] (i.e. implied to be a complete genome, or ≥ 10,000 base pairs long). This set of size-filtered, circularized, more-than-once predicted viruses was dereplicated using mmseqs (95% ANI, 85% breadth required of sequences) to 26,368 viral operational taxonomic units (vOTUs). All vOTUs were annotated using DRAM-v [83], and specifically searched for integrase genes.

DNA density fractionation
DNA was extracted from three biological replicates at each time point using a modified phenol-chloroform protocol adapted from Barnard et al. (2015) [84] as described in [63]. For density gradient SIP processing, 5 µg of DNA in 150 µL 1xTE was mixed with 1.00 mL gradient buffer, and 4.60 mL CsCl stock (1.885 g mL^{-1}) with a final average density of 1.730 g mL^{-1} as described in Sieradzki et al (68).The fractions for each sample were binned into 5 groups based on density (1.6400-1.7039 g/ml, 1.7040-1.7169 g/ml, 1.7170-1.7299 g/ml, 1.7300-1.7449 g/ml, 1.450-1.7800 g/ml), and fractions within a binned group were combined and sequenced. Unfractionated DNA (100 ng) from each soil sample was also saved for shotgun sequencing.

All sequencing was performed on an Illumina Novaseq 2x150 cycles. Pre-aliquoted unfractionated DNA from each sample was sequenced to an average of 20 Gb per sample, and DNA from each density fraction was sequenced to an average of 10 Gb per fraction, yielding a total of 227 metagenomes. Illumina adapters and phiX were removed using BBTools and reads were quality trimmed using Sickle using default parameters.

Metagenome assembly, annotation, and binning
To establish MAGs from metagenomes we approached assembly in two ways: 1) co-assembly of unfractionated triplicates for each time point 2) co-assembly of the 5 density fractions from each time point and each replicate. We used MEGAHIT version 1.2.9 for assemblies [66] details described in [63]. Metawrap version 1.3.2 [85] was used to map reads from unfractionated metagenomes to contigs from each assembly, bin each assembly with MetaBAT2 [73] and Maxbin2 [72] and refine bins. Genomic bins from all samples as well as bins from soil

metagenomes collected at the same site in the preceding winter [37] were then dereplicated at 95% average nucleotide identity (ANI) using dRep version 3.0.1 [76] to create a final collection of high quality 503 metagenome assembled genomes (MAGs) that were on average 87% complete and 5% redundant. Taxonomy was assigned to bins using GTDB-tk version 1.5.1 [86].

To calculate abundance measurements for MAGs, reads from unfractionated samples were mapped back to the MAG collection using bbmap with minid=0.98 (https://jgi.doe.gov/data-and-tools/bbtools/). Mapping statistics were then used to calculate coverage at reads per kilobase million (RPKM), mapped read counts and breadth of coverage using CoverM (https://github.com/wwood/CoverM), and were normalized to sequencing depth.

Calculating relative abundances of the vOTU collection
To quantify abundance of vOTUs in viromes and metagenomes and to assess activity via qSIP we mapped reads from these sequencing efforts to our vOTUs. All reads from viromes, metagenomes, and SIP-fractionated metagenomes were mapped to the set of vOTUs using bbwrap.sh at 98% minimum identity. Samtools [87] sort and index functions were applied to resulting bam files. We used CoverM to calculate breadth and read count per vOTU per sample. Read counts were divided by total reads per sample to calculate relative abundance. For virome relative abundance we considered vOTUs present in a sample if they had at least 80% breadth covered (fraction of genome covered by reads). For use with the qSIP pipeline, we found that few vOTUs had reads that mapped stringently (98% identity) and in all three replicates of multiple density fractions in both ^{18}O and ^{16}O conditions and therefore chose a lower breadth cutoff, 50%, for detection of vOTUs in SIP fractions (described below).

Ordination plots
To understand compositional differences through time responding to rewetting we constructed ordination plots. For MAGs we constructed a matrix of metagenome relative abundance per sample per genome. Similarly for vOTUs, we generated a matrix of relative abundance per sample per genome, using vOTU relative abundance as calculated from our virome samples. We used the python scikit package [88] to calculate Bray-Curtis dissimilarity and to perform principal coordinates analysis (PCoA) to visualize the dissimilarity between samples.

Virus-host linkage and assigning viruses a host taxonomy
To link vOTUs to potential host microbial MAGs, we used multiple approaches, starting with CRISPR spacer searches. We predicted CRISPR arrays using minced (https://github.com/ctSkennerton/minced) [89] in the original set of MAGs (not dereplicated) from this study, in MAGs from another qSIP study conducted in a soil from our HREC field site [37], and in our viromes. 84 MAGs and 32 vOTUs contained CRISPR arrays with at least 1 spacer. We aligned the MAG spacers against the vOTUs using BLASTn [90], and vice versa, and screened for hits with no more than one mismatch and no gaps between the full spacer and the vOTU. By these criteria, only one vOTU spacer matched a MAG in our dataset. This vOTU appeared in two of three plots and in two time points for each plot. In contrast, 25 MAG spacers from 6 MAGs matched 19 vOTUs. From these linkages we assigned host taxonomies to vOTUs using the associated MAGs GTDB taxonomy [86].

To assign host taxonomy to additional vOTUs we combined these CRISPR spacer searches in MAGs, with a broader set of CRISPR spacer matches, and contig taxonomy predictions. Using Kaiju [91], we assigned a consensus host taxonomy per vOTU. In addition to MAG and vOTU spacers, we also predicted spacers in unbinned metagenome sequences using minced and established contig taxonomy for these unbinned sequences using Kaiju. We used the same BLAST parameters to match these unbinned CRISPR array spacers to our dereplicated vOTU

set. Next, we queried the comprehensive spacer database generated in Shmakov et al. 2017 [92] against our vOTU sequences using the same BLAST parameters. Each spacer from this database [92] included an NCBI taxonomy that was assigned to matching vOTU protospacers.

We also used vOTU sequences to inform host taxonomy. Previously, Al-Shayeb et al. 2020 and others assigned host phyla to phages based on whether ORF annotations in phages were predominantly of one phylum [93]. Here, we used Kaiju on vOTUs to assess taxonomy. Most vOTUs were assigned to microbial taxonomies that presumably reflect shared host-virus genome/gene content. We used this microbial taxonomic assignment to set a putative host. For vOTUs predicted to have viral taxonomies we captured host lineages using the Virus-Host Database [94].

Lastly, we created a database of all vOTUs, their host prediction, and the source of the host prediction – CRISPR spacer-based taxonomy from GTDB for MAGs, unbinned spacers with Kaiju taxonomic predictions, NCBI taxonomies from spacers matched from the spacer database used, or Kaiju taxonomy predictions per vOTU. We used this database to determine the consensus taxonomy between these sources closest to a species level by searching for the greatest common denominator. This allowed us to find putative hosts for 93.1% of total vOTUs at the domain level, and 92.8% at the phylum level.

Examination of evidence for viral induction
To quantify viruses in our system that were present both as prophages in MAGs and as VLPs in the virome we mapped virome reads to metagenomes and looked for alignment between metagenome sequences and vOTUs. Specifically, we mapped all virome reads to metagenome assembled sequences at 90% average nucleotide identity. We used coverM (https://github.com/wwood/CoverM) to generate breadth and coverage calculations for mapped reads and identify metagenome contigs that had virome reads mapping with at least 1000 bp covered by reads, but not mapping with 100% breadth. We believed this implied that reads mapped to a potential lysogenic viral genome embedded in the host genome. Using BLASTn [90], we aligned the set of metagenome contigs that met these criteria against our vOTUs with a minimum E-value of 10^{-100}. We subsetted the resulting matches to vOTUs that matched a metagenome contig with greater than 90% nucleotide identity, aligned with a metagenome sequence that had more than 10 Kbp of flanking region around the alignment, and an aligned section of at least 10 Kbp. This resulted in 11 vOTUs representing candidate lysogenic viruses. Using ggKbase (https://ggkbase.berkeley.edu/), we manually analyzed each of these vOTUs and their corresponding metagenome contigs for aligned and unaligned regions consistent with phage (enriched for hypothetical genes, viral structural genes, integrase genes). This resulted in two sequences that appeared to be lysogenic: found both as vOTUs in viromes and in metagenomes in the context of bacterial sequences.

Assessment of prophages in MAGs
Prophages were identified from our set of MAGs by virSorter version 1 categories 4 and 5 [77], or by VIBRANT [79]. Active prophages, i.e. prophages assessed as replicating more than their flanking host genome, were identified by running PropagAtE [95] with metagenome read mapping files to MAGs previously generated. PropagAtE relies on differential coverage between prophage and adjacent host regions.

Viral response categories
To establish viral response patterns through time, we established the set of 6,840 vOTUs present in a specific plot for three or more time points; we refer to these as “persistent vOTUs.” Persistent vOTUs represented an average of 11% of the total virome reads through time. We

generated hierarchically clustered heatmaps (cluster maps) per plot in seaborn [96] using relative abundances per time point for each vOTU. With cluster map observations and k-means clustering, we established 5 response categories based on vOTUs presence or absence in given time points: 1) 'early vOTUs' present at 0h, 3h, or 24h post wet-up; 2) 'late responding vOTUs' present at 48h, 72h, or 168h post wet-up; 3) 'ubiquitous vOTUs' present in all time points; 4) 'vOTUs present at 0h and 168h' and one other time point; 5) 'other' vOTUs that did not fall into these categories. We summed vOTU relative abundances across these categories for each time point per plot. We used the seaborn relplot function [96] to visualize response categories through time per plot. To measure the host signal by response category, we summed the unique vOTUs of a given bacterial putative host phylum or domain per category. We visualized host abundances per response category by overlaying seaborn swarmplots on boxplots where each point corresponds to a field plot.

Construction of integrase relative abundance and richness barplot
We used the seaborn relplot function [96] to construct graphs of vOTUs that did (4463 unique vOTUs) or did not contain integrase genes. We plotted the set of vOTUs split into these two categories and by circular versus linear, by their aggregated relative abundance through time and by vOTU richness per category through time.

Quantitative stable isotope probing
Atom percent excess (APE) isotopic enrichment values were calculated using quantitative stable isotope probing (qSIP) [35, 37, 63] by normalizing MAG and vOTU relative abundance to the quantity of DNA per density fraction [37]. Both bacterial and viral genomes were required to be detected in all three replicates of each labeled ^{18}O treatment and in three replicates of unlabeled (^{16}O) treatments for the bootstrapped median atom percent excess (APE) to be calculated per genome. In the qSIP output we removed genomes with a lower APE median confidence interval < 0 (i.e., not statistically significant), and ranked the remaining 75 MAG and 177 vOTU genomes first by time and then by descending APE value. We identified the first timepoint each genome appeared as enriched and constructed ranked APE curves using the seaborn python package relplot [96]. To compare MAG and vOTU enrichment dynamics, we calculated the mean differences in rank of isotopically enriched genomes (relative to each previous time point). We plotted median APE values per MAG and vOTU through time for our most prevalent vOTUs and hosts – Actinobacteria, Alphaproteobacteria, and Gammaproteobacteria – using seaborn line relplots. We calculated the ratio of vOTU to MAG enrichment by summing the median APE values of vOTUs and MAGs per phylum and using MAG aggregated enrichment as the denominator.

Viral contribution to microbial mortality
We modeled the viral contribution to microbial mortality using a range of potential burst sizes (virions per infected cell) to relate the number of approximated infectious viral particles through time to observed microbial cell death counts. Counts of microbial cell mortality were derived from our previous qSIP analysis of corresponding amplicon sequence data [63]. We used the median rate of rRNA copies lost per gram soil per day and converted this rate to per gram soil by multiplying by the number of days. To convert rRNA copies to cells lost, we used a conservative assumption of six rRNA copies per microbial cell [97]. The approximate loss of microbial cells per gram of soil was used to represent the total observed microbial mortality. To calculate the contribution of viruses to observed mortality, we estimated the number of total virions per time point, using the mean aggregated relative abundance across plots (total reads mapped to our vOTU dataset). We used the fraction of viral reads to estimate viral DNA of total extracted DNA per time point per plot. With our estimate of viral DNA and a mean genome

length of 2.1254 x 10^4 bp, we used equation 1 to estimate plasmid copy number to calculate virions per time point:

$$\text{Virions} = \frac{\text{X ng} \times 6.0221 \times 10^{23} \frac{\text{molecules}}{\text{mole}}}{\text{N} \times 660 \frac{\text{g}}{\text{mole}} \times 1 \times 10^{9} \frac{\text{ng}}{\text{g}}} \quad (1)$$

$$X = Calculated\ viral\ DNA$$

$$N = Average\ calculated\ genome\ length\ (bp)$$

As an average viral burst size in soils is unknown, we converted number of virions to cells lysed by using a range of viral burst sizes from one virus released per cell [54, 98] to 1000 [99]. Virions scaled to cells dead by the burst size range served as a numerator for viral contribution to microbial mortality calculated with equation 2. We next captured cumulative viral contribution to microbial mortality through time by taking the cumulative sum of all previous time points for each time point.

$$Viral\ contribution\ to\ microbial\ mortality = \frac{Virions\ \times\ burst\ size}{\frac{degraded\ rRNA\ copies}{6}\ \times\ Days} \quad (2)$$

Our calculations made the following assumptions: 1) All virions detected lyse their host. 2) Virions calculated for each time point represent new infections rather than virions persisting through time i.e., virions were released from newly lysed cells. 3) Our VLP-virome extraction protocol efficiently extracted 100% of soil viruses, i.e., viruses detected represent all possible soil viruses. 4) The mean vOTU genome length represented an accurate approximation of soil viral lengths irrespective of short read metagenomics and potential assembly fragmentation. Our data supported the second assumption given that only a minority of vOTUs appeared in multiple time points (Supplementary Figure 2). Further, we performed a sensitivity analysis of the impact of genome length on our calculation and found a statistically significant relationship between genome length and percent viral contribution to mortality (linear regression on log transformed data, p-value: 6.63 x 10^{-07}) – changing viral genome length by an order of magnitude led to an order of magnitude decrease in the percent contribution to mortality.

RESULTS

Viral Succession

We established the set of MAGs and viral operational taxonomic units (vOTUs) to define the soil microbiome from 15 unfractionated metagenomes over five timepoints and 18 viromes over six timepoints (each in triplicate) generated from California grassland soil collected at the end of the dry season and wet-up in destructively-harvested microcosms (see Methods and our paired study Sieradzki et al. 2022 [63]). We resolved 542 dereplicated metagenome-assembled genomes (MAGs): 503 from total soil metagenomes comprised of diverse soil bacteria and archaea; and 39 from small fraction metagenomes [64] i.e. viral-enriched metagenomes or viromes which represent candidate phyla radiation (CPR) bacteria. This study detected 26,368 dereplicated vOTUs from viromes (26,139) and metagenomes (229) (Figure 1). We consider vOTUs detected in viromes to be extracellularized VLPs, which are distinct from vOTUs detected in metagenomes where analysis cannot delineate between intracellular and extracellular viral populations (Supplementary Table 1). Prior to rewetting, our microbial

community was dominated by Actinobacteria, Alphaproteobacteria, and Gammaproteobacteria [63]. Proteobacteria were abundant, highly active throughout wet-up, and responded early to rewetting. Actinobacteria also were a top-responding lineage to wet-up, but showed less overall activity despite their abundance (see Sieradzki et al., 2022 [63] for more details on the microbial and function response to rewetting).

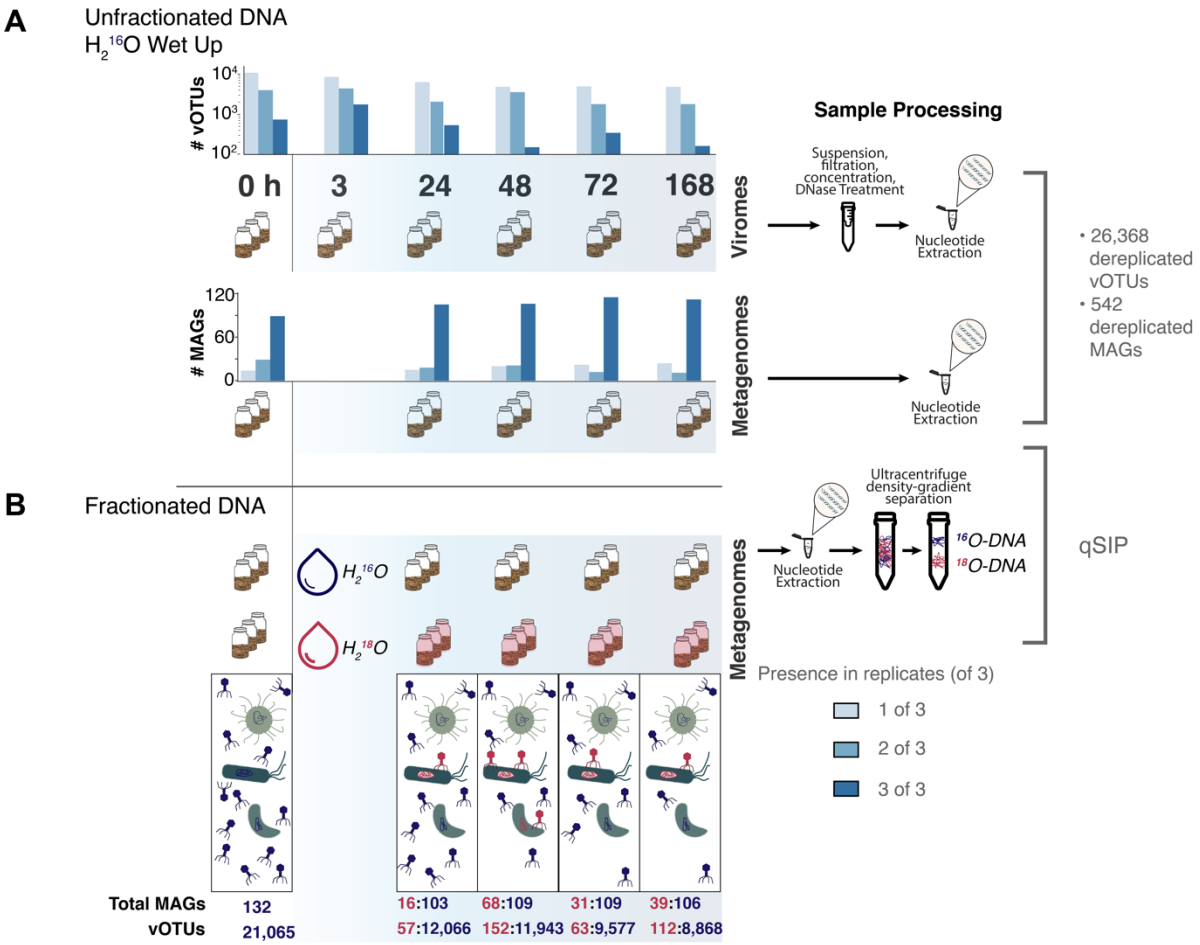

Figure 1 | Experimental overview and analysis of spatial heterogeneity of recovered Genomes from time-resolved cellular and viral size-fraction metagenomes following soil wet-up. (A) Triplicate sampled soil microcosms were destructively harvested before (0h) or following addition of natural abundance water ($H_2{}^{16}O$) (3h, 24h, 48h, 72 and 168h) for the generation of viromes and metagenomes. Microcosms fated for metagenomic sequencing did not include a 3h time point. Associated barplots visualize the number of (top) recovered vOTUs (log scale) or (bottom) MAGS found in one (lightest blue), two, or three (darkest blue) of three replicate microcosms. **(B)** Stable isotope probing (SIP) incubation: $H_2{}^{16}O$ or $H_2{}^{18}O$ (in red) were added to triplicate microcosms (no 3 h time point), which were then density-separated prior to shotgun sequencing. Below is a cartoon demonstrating that viral isotopic incorporation relies on microbial assimilation of ^{18}O into DNA. The associated counts show the total number of enriched MAGs and vOTUs (in red) relative to the total number of MAGs and vOTUs (blue) detected at each time point.

To explore spatial heterogeneity of viruses and potential hosts, we analyzed the number of unique vOTUs and MAGs detected in all three, just two, or only one of the three biological field replicates (Figure 1A). MAGs, predominantly representing bacteria, were more evenly detected (present in all three replicates) throughout soil replicates compared to vOTUs, and throughout

time. In contrast, vOTUs were more likely to be detected in a single replicate than in all three, by an order of magnitude or greater (Figure 1A).

To visualize the spatial and temporal succession of microbial and viral populations, we calculated ordinations based on the Bray-Curtis dissimilarity of relative abundance of MAGs (Figure 2A left) and vOTUs (Figure 2A right). The first two ordination components of MAG abundances revealed that succession of potential hosts was most pronounced over time (52.54% variance explained) with a minor spatial component and explained in total over 70% of the variability. On the contrary, abundances of viruses had a significant spatial component, with the first two time points (3h and 24h) clustering with time 0h in two of the three plots. The first two ordination components of vOTUs represented a smaller fraction of the variance compared to potential hosts (35.6%).

Following rewetting, we found that viral richness significantly decreases, while viral biomass significantly increases. Early time points showed higher richness of vOTUs, but with lower abundances per vOTU (Figure 2B, Figure 2C). In contrast, later time points, in particular 168h, shifted to a less even viral community, with higher relative abundances of fewer vOTUs. Average vOTU richness, as measured through the number of unique vOTUs per time point, decreased significantly after 3h (linear regression – pvalue: 0.02; rvalue: -0.53) (Figure 2B). While the number of vOTUs decreased by nearly 50% one-week post wetting, viral biomass increased by at least five-fold (Figure 2D). We found viral biomass, as proxied by calculating viral DNA through time, statistically significantly increased by the end of the time sampled (linear regression – pvalue: 2.1×10^{-3}; rvalue: 0.68).

To further characterize viral temporal succession, we focused on the set of vOTUs that were present in at least three time points within each replicate. We termed these persistent vOTUs. Previously, our group observed that at sub-phylum taxonomic levels microbial response to wet-up is sequential with rapid, intermediate, and delayed responding groups [14]. We predicted that persistent vOTUs would reflect host dynamics and show similar temporal response patterns. For each replicate-specific set of vOTUs we constructed hierarchically clustered heatmaps of relative abundance to establish vOTUs that behave similarly across wet-up (Supplementary Figure 1). This clustering demonstrated several broad patterns of abundance dynamics consistent across replicates: 1) vOTUs present early in wet-up (0h, 3h, 24h) that then disappear or drastically decrease in abundance i.e. early vOTUs; 2) vOTUs that appear for the first time 48hafter wet-up, i.e. late responding vOTUs; 3) vOTUs that are present across all time points throughout the wet-up, i.e. ubiquitous vOTUs; 4) vOTUs that are present in dry soil (time 0) and at the end of the wet-up time course (168 h), but are not detected in all time points in between, i.e. 0h and 168h vOTUs. vOTUs that did not fit into these categories were included in the “other” category (Supplementary Figure 2A). Each of these defined response categories represented, at times, up to 15% of the total virome reads. Overall, we observed that viruses follow plot-specific successional patterns to wet-up.

We were curious whether late vOTUs (first detected as VLPs at 48 hours) were derived from viral infections occurring at earlier time points. We predicted that these vOTUs could be found in the metagenomes and tested this by asking if these vOTUs were inside microbial cells or harbored in host chromosomes. However, metagenome reads from time points 0h and 24hdid not map to late vOTUs (Supplementary Figure 3). We were unable to trace vOTUs observed as VLPs following 48 hours from metagenomes collected prior to VLP detection.

In previous work and in our paired study, we observed that Actinobacteria and Proteobacteria dominate the microbial post wet-up response [8, 14, 63]. We hypothesized that the vOTUs

would reflect these host responses. While we appreciate that a phylum-level host analysis of viruses does not reflect known viral host ranges (which is often on a strain level) [10, 100], wet-up shows consistent phyla-level microbial responses and our host predictions for viruses were limited to a coarse taxonomic view. Thus, we examined the vOTU putative host composition within each taxonomic group (Supplementary Figure 2B) and found vOTUs infecting Actinobacteria dominated the groups responding immediately and after 24 hours. Alphaproteobacteria-infecting vOTUs were the second most numerous and were also captured in groups on both timescales. In contrast, the early vOTU category was equally dominated by Alphaproteobacteria- and Actinobacteria-infecting vOTUs. Generally, vOTUs with no host assignment (unknown) comprised 6 to 47% of total vOTUs, with the largest proportion found in the ubiquitous vOTU category. Overall, we did not find evidence for our hypothesis: vOTUs sampled in each time frame were not predicted by the patterns of their hosts. Rather, vOTUs of prevalent hosts in our system (Actinobacteria and Proteobacteria) appeared as the most prevalent vOTUs in each response category.

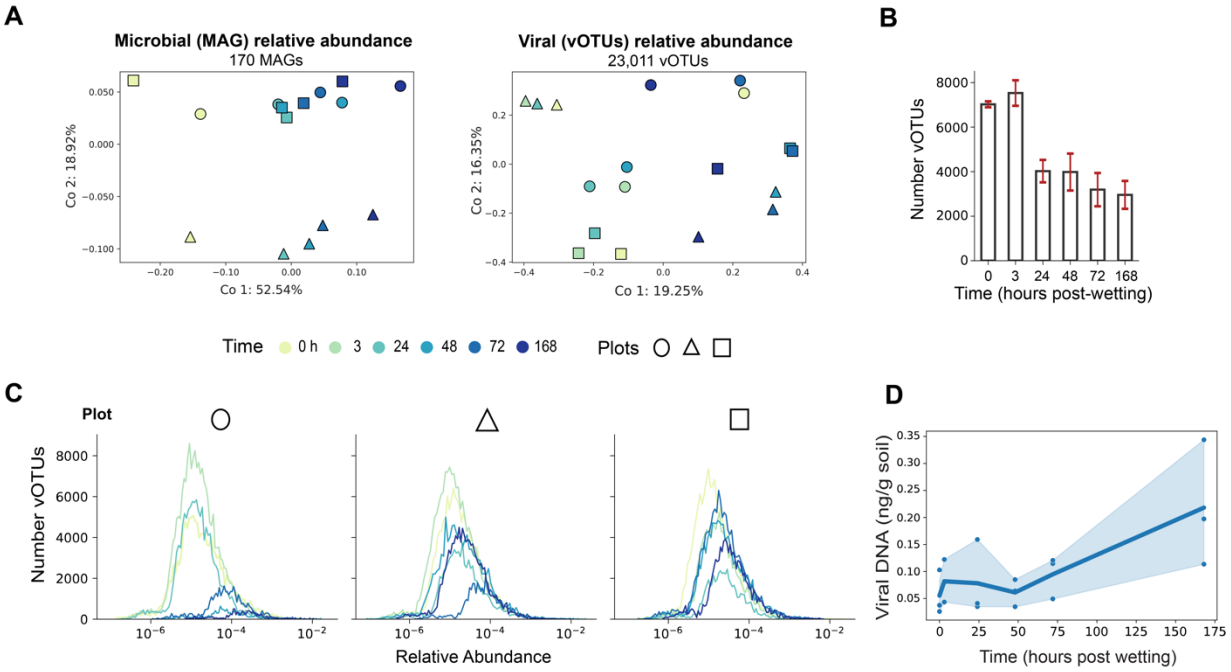

Figure 2 | Temporal compositional changes in microbial and viral communities following soil wet-up. **(A)** PCoA plots of MAGs (left) and vOTUs (right) calculated based on Bray-Curtis dissimilarity colored by time with different marker shapes signifying distinct field plots (biological replicates). **(B)** Barplot of the mean total number of unique vOTUs per time point. Error bars (red) show standard error of mean across all three field plots. **(C)** Distribution of vOTU relative abundances per time point (colored curve) graphed by field plot (signified by shapes used in A). The y axis is the number of unique vOTUs detected per time point per plot. **(D)** Viral biomass approximated by total extracted viral DNA (ng) per gram of soil plotted through time. Each point represents a distinct microcosm. The shaded area around the line represents a 95% confidence interval.

Characterizing Active vOTUs with SIP metagenomics

After analyzing the dynamics of the total set of viruses following rewetting, we investigated the subset of viruses actively replicating at any time to evaluate the impact of viruses on their microbial host abundances. Actively replicating viruses here are defined by incorporating ^{18}O

from the $H_2{}^{18}O$ wet-up (Figure 1). Specifically, we applied qSIP to calculate isotopic enrichment (atom percent excess, APE) of DNA, which is a proxy for genome replication rate [37, 101]. For MAGs and vOTUs we constructed rank curves sorted by APE and time using taxa with APE significantly greater than zero (Figure 3). This enabled us to quantify each genome's isotope incorporation, or growth, through time and simultaneously the overall pattern per time point. 1) In the first time point, we show rank curves for genomes detected as enriched. In subsequent timepoints, the genomes from the first time point remain in the same rank position, and any new genomes appearing as enriched are presented in the same Figure to the right of the previously detected active genomes. 2) the disordering of previous time points' APE ranked curves in a time-dependent manner i.e., the MAG and vOTU APE change at a taxon-specific level through time resulting in the disruption of the descending rank pattern in later time points (Figure 3). The disordering seen in these plots represents the changes through time of a genome's enrichment. For instance, a genome first detected as highly enriched at 24 hours, may decrease in its enrichment by 72 hours and while its x-axis position remains the same throughout the time course, its APE value reflected on the y-axis thus becomes lower than its expected initial rank. Also, a genome that was previously detected as enriched, may become undetected, this is visualized in the density of a curve becoming sparser as it is missing the points that represent previously detected genomes.

For both MAGs (Figure 3A) and vOTUs (Figure 3B), we found the greatest number of newly isotope-enriched genomes at 48h. MAGs most isotopically enriched when they first appeared remain among the most enriched genomes if they are detected in later time points. Despite MAG and vOTU enrichment similarities, by 168 hours there is a higher degree of disordering amongst vOTUs than that of the MAGs. vOTUs most highly enriched at 24h and 48h (≥ 20 % APE) [63] in the time course appear much lower than their initial rank or are altogether undetected, and vOTUs first appearing as slightly enriched become more enriched at subsequent time points (increase in APE relative to their x-axis position) – the average change in rank from 24 hours for vOTUs is 38 and for MAGs is 9. Actinobacteria-infecting vOTUs are the most numerous active viruses across time points. However, the most highly enriched vOTUs vary through time and are predicted to infect Proteobacteria or have an unknown host (Figure 3B). Proteobacteria MAGs are also the most highly enriched microbial genomes, implying a high growth rate. Enriched archaeal viruses are detected at each timepoint with the largest number detected at 48h. Further, the ratio of isotopically-enriched viruses compared to microbes changes through time (Figure 1B, bottom panel): at 24 hours there are three times as many viruses as bacteria, at 48 hours only twice as many, and by 168 hours that number increases to 2.7 more active viruses to microbes.

Of the 177 total enriched vOTUs detected in metagenomes, 58 are found in VLP viromes, indicating that at least 33% of genomes replicating and assimilating isotope within host cells are also able to escape their host cell to be detected as putative virions.

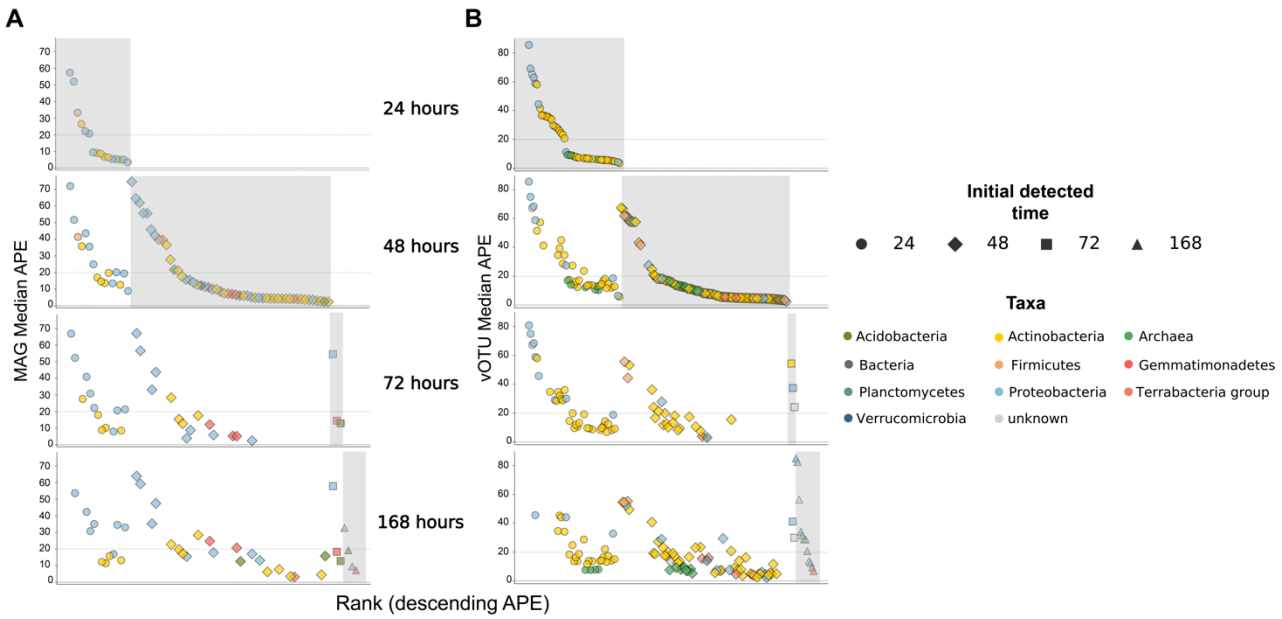

Figure 3 | Changes in abundance of isotope-enriched (growing) viruses and microbes through time following soil wet-up. Rank abundance curves of atom percent excess (APE) ^{18}O wherein the x axis shows absolute rank of genomes sorted first by time and then by descending APE value, and the y axis shows the median APE per genome of **(A)** microbes (MAGs) and **(B)** viruses (vOTUs). Colors represent taxonomic groups. Shapes indicate the time point a genome first appeared as isotope-enriched. Gray regions represent genomes appearing as newly enriched in a given timepoint.

Viral lifestyle characterization

To further assess how viruses may control host populations during soil microbiome assembly we investigated temperate capabilities of vOTUs. To test our hypothesis that wet-up induces temperate phages we searched for vOTU genomes common to viromes and metagenomes that contained bacterial flanking regions in metagenomes to discover and quantify lysogeny in our system. This strategy yielded just two candidates of vOTUs found both as VLPs in the virome and as putative prophage in metagenome contigs and only one of these candidates was successfully binned into a MAG. The unbinned sequence was predicted to be an Alphaproteobacteria, *Rhizobium leguminosarum*. The MAG identified as having a prophage was a Gammaproteobacteria of the genus *Pantoea*. In this study we did not further characterize this binned putative prophage since it was only detected in one of the three plots at two non-consecutive time points (0 and 24h).

Unsuccessful in finding vOTUs appearing as both integrated in MAGs or bacterial sequence and as VLPs, we examined our system for temperate phage by analyzing the genomic capacity of vOTUs to integrate, via an integrase gene, into a host chromosome (Figure 4). Of the total vOTUs detected 16.9 % (4,463) contained an integrase gene and were denoted as putative prophages. Concerned that vOTU contigs may be partial viral genomes left fragmented during assembly, we split the results of integrase-encoding and -absent viral genomes by vOTUs that circularize, implying genomic completeness, and vOTUs that are linear, and thus may or may not be complete. We reasoned that if the linear set of vOTUs followed similar trends to

complete, circularized vOTUs, then the patterns displayed would be representative of biological trends rather than artifacts of incomplete assembly of linear vOTUs.

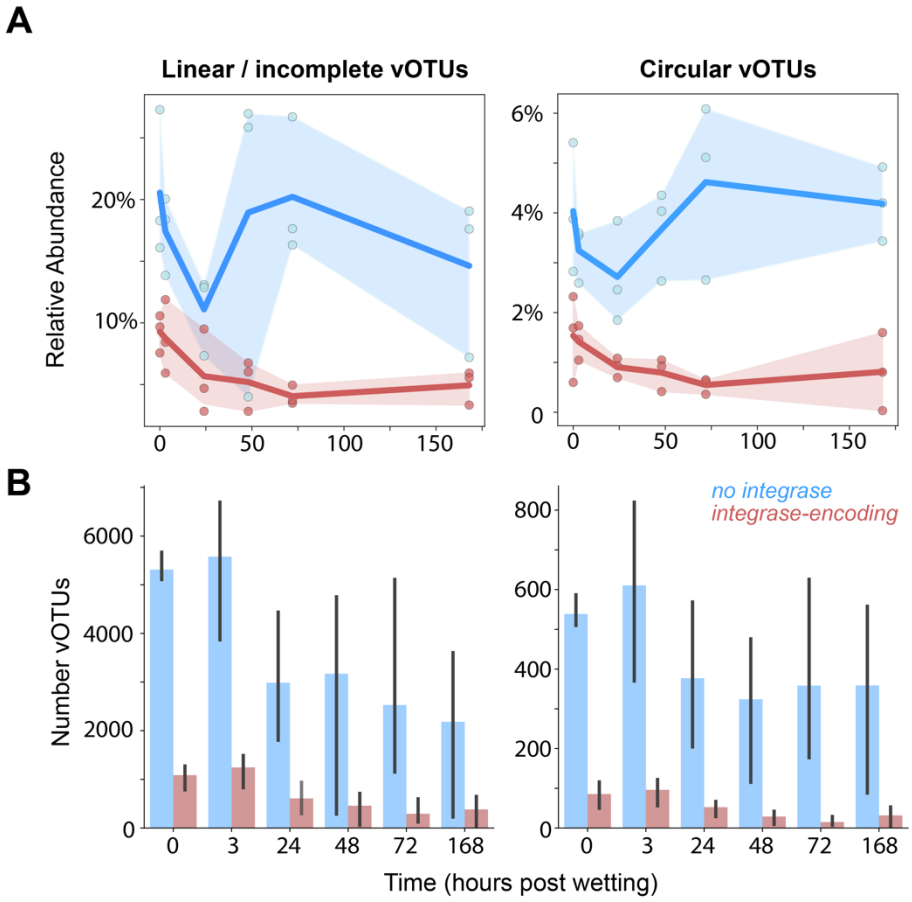

Figure 4 | Relative abundance and richness of integrase-encoding vOTUs through time following soil wet-up. vOTUs were split by whether they encode an integrase gene (red) or not (blue) and whether the vOTU is predicted to circularize (right set of graphs) or is linear and perhaps fragmented (left set of graphs). **(A)** Aggregated relative abundance (percent of total sample reads) of integrase-encoding or not integrase-encoding vOTUs. **(B)** Counts of integrase-containing and non-integrase containing vOTUs.

For both linear and circular vOTUs, non-integrase encoding vOTUs represented a greater relative abundance of the total virome community, more than twice as much at most time points (Figure 4A). Further, up to five times more circular and linear vOTUs did not contain compared to containing an integrase gene (Figure 4B). Integrase-containing vOTUs showed the same trend in relative abundance over time in both linear and circular vOTUs: a steady decline in relative abundance in the first 48 hours and then relatively constant abundances through 168 hours (Figure 4A). There does not appear to be an increase in integrase-encoding vOTUs following wet-up. The richness data underscore this. Both the number of integrase-encoding vOTUs and non-integrase containing vOTUs are consistent whether looking at linear or circular vOTUs. The non-integrase encoding vOTUs are not only much more numerous, but also, they reflect the pattern of total dereplicated vOTUs through time (Figure 2B) – a decrease in count through time.

We also tested whether vOTUs appearing after wet-up (0 h) were enriched in integrase genes, with the logic that vOTUs appearing for the first time following wet-up may be prophage excising from genomes. The post-wet-up vOTUs were not significantly enriched in integrase genes compared to vOTUs in the dry soil (Chi-square test – statistic: 1.6; pvalue: 0.2).

To further support the inference that wet-up does not induce temperate phages, we took a MAG-centric approach. We used bioinformatic tools that can predict prophages in the context of bacterial genomes, here MAGs, to discern whether, how many (counts), and how prevalent (abundant) prophages are in this system (Supplementary Figure 4). We looked at both aggregated relative abundance across all time points of MAGs by phylum and count of total MAGs with or without prophages. Most phyla contained a predicted prophage, but prophage-containing MAGs for each phylum were both fewer and less abundant than MAGs without detected prophages. For lineages other than Actinobacteria and Alphaproteobacteria, just one to six MAGs per phyla contained prophages. The aggregated relative abundance data underscores this point as the abundance of MAGs containing prophages (Supplementary Figure 4a) was lower than the proportion of the number of MAGs containing prophages (Supplementary Figure 4b). MAGs containing prophages comprised 15-26% of the total abundance of Actinobacteria and Alphaproteobacteria per time point. Based on coverage differences between the prophage sequence and the flanking host genomic regions [95] we identified only three prophages that seemed to be actively replicating. One of these prophages appeared active at all time points in at least two out of the three replicates, and was integrated into a MAG of Alphaproteobacteria genus *Microvirga*. The other two prophages were active only in a single replicate and in either one or two time points, and were integrated into genomes of Actinobacteria family Gaiellaceae and Alphaproteobacteria family Xanthobacteraceae, respectively.

To further investigate viral lifestyle and assess whether VLPs correspond to lysis we looked for evidence for non-lytic viruses i.e. inoviridae in the studied soils. We performed an HMM search using the pI-like ATPase protein family HMM, which is conserved in filamentous inoviruses [102], and found no evidence of inoviridae in these data.

Virus-host dynamics

We next examined the dynamics of viruses in a host-dependent manner to test whether and to what extent viruses may serve as a top-down control during community assembly. Given the prevalence of MAGs and vOTUs with a taxonomy or host-level taxonomy assignment of Actinobacteria and Proteobacteria, and given the previous high degrees of mortality and growth following wet-up calculated for bacteria of these phyla [8], we focused analyses comparing vOTUs and MAGs to these lineages. Specifically, within Proteobacteria we focused on Alpha- and Gamma-proteobacteria as growth could not be detected for other classes within this phylum in our experiment. We analyzed APE for Actinobacteria, Alphaproteobacteria, and Gammaproteobacteria MAGs and found that individual MAGs mostly show a similar trend of increasing in enrichment in the first 48 hours (Supplementary Figure 5A). The Proteobacteria MAGs show a higher overall degree of enrichment for individual MAGs than the Actinobacteria (Supplementary Figure 5A). Similar to the temporal pattern of enrichment, the number of enriched MAGs increased over the first 48 hours, decreased through 72 hours, and mostly stabilized until the end of the time sampled for Actinobacteria and both Proteobacteria lineages (Supplementary Figure 5D). For both phyla, there were higher counts of enriched vOTUs than enriched MAGs. At 24 hours, for instance, there were more than twice as many vOTUs as MAGs for all lineages, and for Actinobacteria in particular, over fifteen times as many vOTUs were detected as enriched compared to MAGs.

Viral-OTUs, overall, showed a similar pattern of enrichment to that of MAGs: increasing over the course of the first 48 hours, decreasing in APE through 72 hours, and stabilizing or slightly increasing their APE by 168 hours (Supplementary Figure 5B). For putative Actinobacteria-infecting phages, the majority of vOTUs clustered into a low activity region (less than 20% APE [63]) which is composed of two subgroups. A separate cluster of higher activity vOTUs (36% of the total) showed APE values consistently above 20 %, but did not follow clear trends through time. Alphaproteobacteria- and Gammaproteobacteria-infecting viruses showed similar trends in APE through time that appear as denser regions in their vOTU median APE plots.

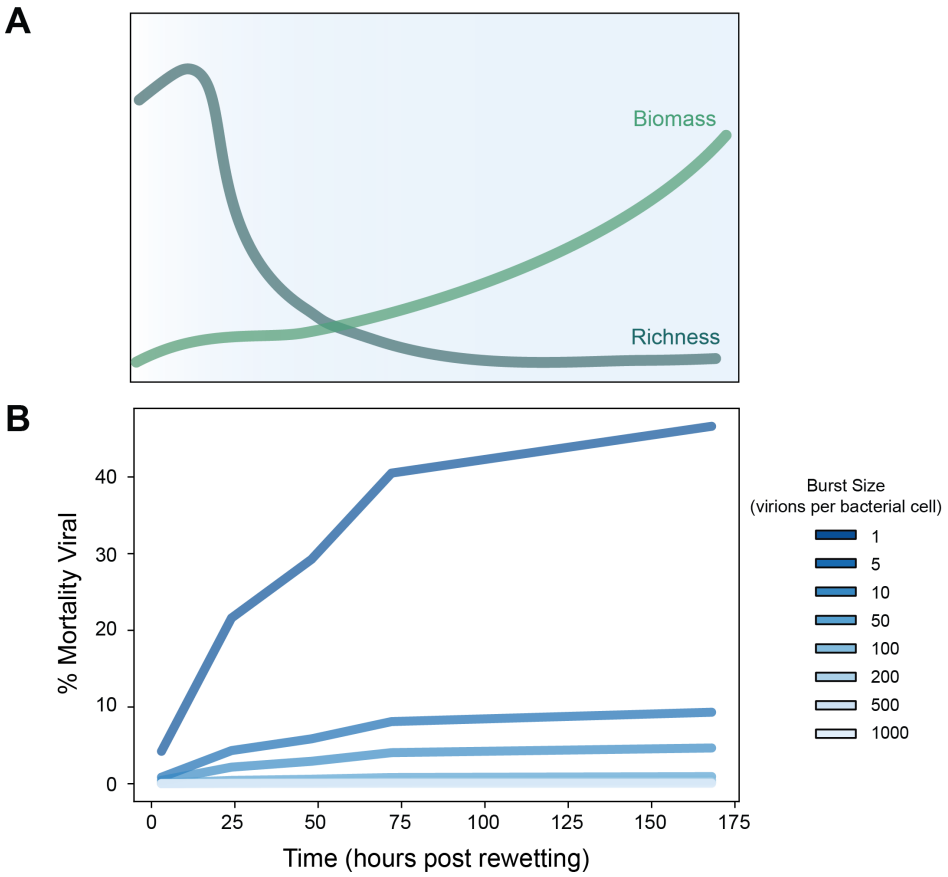

Figure 5 | Viral response to wet-up and corresponding contribution to microbial mortality. (A) Conceptual model of changes in viral richness (gray-blue) and biomass (green) over time. **(B)** Modelled contribution of viruses to microbial mortality where each line graphed represents an estimated percent contribution for a different viral burst size shown in the legend ranging from 1 virion per lysed microbial cell to 1000 virions per lysed microbial cell.

To understand phylum-level dynamics between vOTUs and MAGs we examined the ratio of vOTU and MAG median APE values (Supplementary Figure 5C). Actinobacteria vOTUs had the highest ratio APE relative to hosts through time as compared to the Proteobacteria lineages, and only Actinobacteria viral enrichment was greater than MAG enrichment (ratio >1) observed in the first 48 hours. For all lineages, vOTU enrichment outpaces MAG enrichment (observed as

positive slopes in Supplementary Figure 5C) between 24 and 48 hours, and again at 72 hours for Actinobacteria and Alphaproteobacteria.

The dynamics of MAGs and vOTUs are also reflected in the counts of active genomes detected through time (Supplementary Figure 5D). Viruses and MAGs showed similar temporal trends for isotopic enrichment (APE) and active genome richness (number of APE-detected genomes). We similarly analyzed other phyla using these metrics of MAG APE, vOTU APE, number of enriched genomes through time and found no discernable patterns.

Quantifying viral contribution to microbial mortality

We approximated the viral contribution to mortality following wet-up using VLP sequence data from this work and bacterial mortality estimates from corresponding SIP-density fractionated amplicon sequencing [63]. We modeled a range of viral burst sizes from one virus released per cell lysed [54, 98] to 1000 viruses released per cell lysed [99]. Taken cumulatively, looking at viral lysis of microbes at 3-, 24-, and 48-hours following rewetting, viruses account for minimally 0.03% (burst size of 1000) and maximally 29.3% (burst size of 1) of the microbial death observed (Figure 5B). At 168 hours cumulative viral contribution to microbial death ranges from 0.05 % to 46.6 % depending on estimated burst size. We observed at 24 hours the highest per day viral contribution to microbial mortality 0.01 % to 17.4 %.

DISCUSSION

The combination of viromes and SIP enabled identification of pools of viruses and their dynamics during the community restructuring after soil was rewet after a long dry summer period. We 1) assessed viral biomass and richness following rewetting and posited that dry soil may serve as a seedbank of virions for the growing season; 2) analyzed dynamics of active viruses and found these more closely follow host populations rather than control them; 3) investigated viral life cycle and observed minimal evidence for lysogeny suggesting lytic lifestyle is predominant in soil viruses; 4) estimated viral contribution to microbial mortality to discover viral contribution to steadily increases following rewetting; 5) examined viral succession and found that spatial heterogeneity drives temporal trajectories.

Dry soil serves as rich seedbank of viruses of which active viruses follow rather than control hosts

We observed a large decline in viral richness, and by extension diversity, in the first 24 hours following rewetting, which was inversely related to an increase in viral biomass (Figure 5A). This pattern was consistent across all soil replicates making it detectable despite the high degree of inter-sample heterogeneity. We thus observed that only a subset of viruses present in seasonally dry soil thrive following rewetting. Intriguingly, analysis of the total viral pool present after wet-up did not reveal patterns of succession correspondent with known host response previously reported or observed in our study (Supplementary Figure 2-3) [8, 14, 63]. Shifting focus to the active subset of microbial and viral populations (Figure 3, Supplementary Figure 5) revealed vOTUs to behave more similarly to their active hosts based on the number, types, and degree of isotopic enrichment of genomes through time.

Marine system studies have shown that viruses follow their hosts' dynamics [103] and that high local diversity of viruses may be drawn from a seedbank of nearby viruses [18]. Given the richness of viruses in dry soil, we hypothesize that dry soil may be a reservoir, or seedbank, of diverse viruses that become dynamic following rewetting. As suggested in Chow et al. 2014

[103], our isotope targeted results suggest that viral composition follows host dynamics, as opposed to viruses directly controlling host abundance. That is, the total viral pool does not necessarily mirror the total microbial pool, and therefore it is important to focus on the active subset of vOTUs and MAGs to appreciate host-virus dynamics in our soil system.

Our isotopic data revealed a broad diversity of active viruses following rewetting which represent only a subset of the detected viruses in the dry soil seedbank. To investigate viruses that could be important controllers of microbial populations, we categorized the active viruses based on their predicted host phyla. First, focusing on viruses that infect Actinobacteria, we found a range of virus activities. A subset of Actinobacteria viral populations appear to contain a small portion of highly active taxa (>20 % APE), while the majority of Actinobacteria-infecting viruses have a lower level of steady activity (Supplementary Figure 5B). We suspect this small highly active pool of viruses infects the similarly small pool of hosts that fall within the higher activity category. We find similarly structured subsets of varying activity in Alphaproteobacteria, Gammaproteobacteria and the viruses that infect them underscoring the diversity of viral and host activity and response. Across this diversity in activity, we found that viral APE increased faster than microbial APE in the first 48 hours suggesting that these infections happened faster than microbial genome replication (Supplementary Figure 5C). Previously, our group showed in a carbon-SIP experiment that phages can be the most enriched genomes in a soil system [38]. We find here too, Actinobacteria- and Proteobacteria-infecting phages to be the most isotopically enriched viruses that we could identify following wet-up. That is, we can observe in real time, phage replication outpacing bacterial growth in a time- and taxonomic-dependent manner.

We predicted that we would see evidence of virus control on microbial host populations in coupled, offset predator-prey dynamics, but our data suggest that viruses reflect host community dynamics rather than serve as a top-down control on microbial community composition. The relationship of APE through time did not reveal the expected canonical predator-prey paired cycles. Rather, we see that viral enrichment and counts per phylum broadly follow the same trends through time as their bacterial counterparts. Future studies of this system may choose to sample more finely resolved time points [104] to see if predator-prey oscillations may exist more clearly, for example, at 72 hours when we see both virus and host enrichment decrease. However, predator-prey oscillations may only be detected at the species or strain level [100].

Viruses exhibit successional patterns in response to perturbation

Remarkably, we found a consistent successional pattern of our total detected viruses across all plots. However, these successional patterns appeared decoupled from their hosts. Clusters of vOTUs responded similarly across plots (Supplementary Figure 2; Supplementary Figure 3A) – vOTUs found early in wet-up, late-responding vOTUs, vOTUs present throughout the entire time course, and vOTUs that were detected at the start and end of our sampling but not consistently throughout. Within these response groups we observed plot-specific fluctuations and found that the late category of viral response only applies to two of three plots. However, separating viruses into response categories of early, late, etc. echoed the microbial response to rewetting, which shows taxon-specific growth and mortality patterns [8, 14]. We thus hypothesized that these viral response categories would align with previously observed phylogenetic trends for rapid, intermediate, and delayed microbial, i.e., putative host, responses to resuscitation. However, at the phylum level, we did not observe host-specific trends in viral response groups (Supplementary 2B). Rather, host signal within each response category showed the same

trends – viruses of Actinobacteria and Alphaproteobacteria hosts responded early, late, and were ubiquitous across wet-up.

While a clear host signal associated with different viral response groups was not apparent, we found that of Betaproteobacteria-infecting viruses, the mode falls in the early responding category, which is also when Betaproteobacteria have previously been reported to have the highest mortality rate [8]. These results suggest that mortality of Betaproteobacteria immediately following wet-up is driven, in part, by viral lysis. Although it is unclear whether virions detected early in our time course represent recent host infections or whether these virions have persisted from the dry season, our lack of persistent vOTUs suggests virions detected may indeed derive from recent host infections. Our study provides a first glimpse into fine spatiotemporal viral dynamics in soil and enabled us to categorize distinct viral responses to rewetting.

Given the higher spatial homogeneity in microbial distribution and response to rewetting compared to viral distribution (majority of MAGs appear in all samples), it is tempting to hypothesize that this indicates microbes in soil are widely susceptible to infection by many distinct viral populations. However, the lack of specific host-virus linkages in our system meant we were unable to investigate viral host breadth.

Spatial heterogeneity drives viral population dynamics

Our data show spatial heterogeneity is an important feature in understanding the response of viruses to rewetting. While a rapid decline in viral diversity, increase in viral biomass, and successional patterns emerged as trends across the studied soil plots, the majority (59%) of viruses appeared in fewer than three of our total 18 viromes and most do not appear in all biological replicates (Figure 1A). To account for the high degree of spatial heterogeneity we conducted our analyses within each plot as opposed to across all plots which allowed us to uncover emerging trends across space that averages would have precluded. However, comparing viruses to their hosts at this spatial scale posed a challenge because microbes had a more coherent and uniform response than viruses to wet-up. Further, the patchiness of viruses precluded following subsets of viruses through space and time to find statistically meaningful trends. The heterogeneity of soil viruses suggests that infection may not be as uniform across space as potential hosts are. Perhaps, this is the effect of rewetting: virions persisting in soil, more often than not, may be decoupled from their host dynamics, and the addition of water may exacerbate the hurdle of host-viral physical interactions as previous research has predicted increased water potential is associated with lower rates of direct cell-cell contact in soil [105]. On the other hand, wet-up may serve to increase connectivity between soil microsites and relieve dispersal limitations of viruses, supporting host connections. As research has shown in water-undersaturated soils, dispersal is a constraint [106]. Our observed increase of viral biomass following wet-up suggests water would support physical interactions between viruses and their hosts.

The viral heterogeneity observed throughout our field site [107] also underscores our own assumptions in the design of this experiment: that the field plot layout, constructed with our knowledge of microbial distribution across a soil site would enable similar trends for viruses. Rather, our fine-time resolved study and concurrent work studying heterogeneity on a field scale at longer time intervals [107] have compelled us to question what scale of sampling for viruses represents biological replicates. Our results suggest that future studies should consider the distinct scales of microbial and viral populations in soil to have a holistic understanding of microbial communities [108].

We found that each soil plot contained a unique standing community including a seedbank of virions. These viral populations may degrade or thrive following rewetting, but after one week post perturbation we did not observe that viral composition across plots became more similar. Rather, the virions present at the end of the dry season determined the trajectory of the plot-specific viral composition. That is, at this timescale, wet-up is not a perturbation at which we observed a convergence of viral populations across space despite host uniformity at the same sampling (Figure 2).

Scant evidence for lysogeny suggests other lifestyles are dominant

Critical to understanding how viruses impact the soil microbiome during this rapid moment of community response is understanding the mechanism of how viruses live and survive in soil – an analysis of viral life cycle. An emerging idea in soil viral ecology suggests that lysogens are prevalent in soil microbes, and further, lysogeny is a favorable lifestyle for viruses both to remain in association with a host and to weather conditions difficult for growth i.e. dry soil [1, 10–12, 49, 54, 56, 108, 109]. We tested this hypothesis looking specifically at wet-up as an environmental perturbation that could induce prophage and found no evidence to advance this hypothesis.

Our data suggests that vOTUs, which cannot recombine into a host chromosome through an integrase, dominate this system. We found no clear evidence showing wet-up induces a significant number of prophages. The viruses that do increase in abundance following the first 24 hours are predominantly non-integrase encoding. We hypothesized that late-responding vOTUs may also provide a window into viral life strategies (Supplementary Figure 2A) – that examining virome late-responders in metagenomes would reveal these viruses were cell-associated prior to appearance as VLPs. As late-responding viruses did not appear in metagenomes at earlier time points at higher abundances than when they were detected in viromes (Supplementary Figure 3), and prevalent MAGs did not maintain detectable prophages (Supplementary Figure 4), we conclude that temperate phage did not dominate this soil system and they were not the predominant responding viruses to wet-up.

Whether all detected VLPs in our system signify cell lysis remains unclear. While we did not find evidence of inoviridae – viruses that can replicate and release virions without lysing their hosts through a chronic infection [102], other non-lytic lifestyles may be possible. Further, while neither the capacity to integrate into a host chromosome nor persistence as a prophage is prevalent in our wet-up system, we were not able to rule out other mechanisms of viral maintenance in a host cell when a virus is not lytically programmed i.e. pseudolysogeny [110]. Perhaps evidencing the prevalence of pseudolysogeny or some other cell-associated state of soil viruses, the majority (67%) of viral populations detected as active were only found in metagenomes (direct DNA extraction from soil) rather than viromes. For a virus to be detected as enriched it must be infecting host cells to replicate, thus assimilating isotope – most of these active viruses may not be detected as putative virions because of their host-associated state.

Viral contribution to microbial mortality increases though time post wet-up

Microbial death is critical to the flow of nutrients through biomes [1]. A significant feature of soil wet-up is high rates of microbial mortality [7, 8, 16]. Our previous work demonstrated rapid bacterial mortality following wet-up, with 25% of bacteria degrading in the first 3 hours and continued mortality observed through 72 hours [16]. We hypothesized that the initial burst of mortality in the first 3 hours was driven by osmotic lysis due to the rapid change in osmotic pressure, while mortality after 3 hours was driven by viruses or other biological factors [7].

Others have also speculated that viruses play a role in observed mortality following rewetting [111]. We found that viruses play a minor role in mortality in the first 3 hours, when osmotic lysis is likely the dominant mechanism, and the contribution to mortality by viruses increases through time, more than doubling after the first 24 hours (Figure 5B). We estimate that viruses can drive a sizeable portion of microbial mortality in soil – by 168 hours viral-mediated mortality may contribute 0.05 % to 46.6 % of total microbial death dependent on burst size estimated. While our evidence suggests viruses play an important role in microbial mortality following wet-up, we infer that this influence is minimized as wet-up led to a rapid decline of viral particle abundances. If viral biomass continues to increase following 168 hours post wet-up, we posit that the viral contribution to microbial mortality may be higher, and perhaps contribute to microbial mortality on the scale of what is observed in marine systems – lysing up to 20 - 40 % of bacteria daily [112]. There may also be other circumstances in the soil microbiome where viruses play a larger role in mediating microbial death, perhaps in the rhizosphere [38]. Further studies are required to understand a more representative genome length of soil viruses, range of viral burst sizes in soil, and how long VLPs persist in soil to understand whether virions represent recent infections or whether these calculations require SIP techniques to capture an active fraction of viruses. Moreover, viral predation has impacts beyond contribution to mortality broadly. Even low viral turnover rates of key lineages may profoundly impact strain selection and functional potential of soil microbiomes.

Current challenges in the state of the field – linking host and viruses

Using mixed methods and multiple databases we were able to determine at least a domain or phylum-level taxonomy for all but 443 vOTUs (marked “unknown” host). Despite having some degree of host taxonomy resolution for an overwhelming majority of vOTUs detected in our system, we found few CRISPR spacer matches [113] and thus were only able to directly link vOTUs to specific MAGs with high confidence in a few instances. We also used a network-based analysis to connect MAGs to vOTUs modelling canonical predator-prey dynamics, but were unsuccessful in ground truthing these linkages (data not shown). While our methods enabled us to ascertain a host taxonomy for vOTUs and to achieve results that aligned with microbial dynamics on a phylum-level, the current state of host-viral linkage techniques did not allow us to directly implicate viruses as preying on specific MAGs and track predator-prey dynamics on a strain level. However, our host predictions revealed that prevalent viruses in our system infected Actinobacteria and Proteobacteria, which reflected our microbial data: the most prevalent viruses infected the most prevalent hosts.

Others studies have connected viruses to their hosts by combining SIP techniques using specific isotopically-labelled substrates and CRISPR matches which allowed linkages of methanotrophic bacteria to their phages [39]. Further, virus-host linkages may be missed due to spatial scaling issues discussed here which metagenomic studies on soil aggregates or aggregates may reconcile [108].

CONCLUSION

We probed the wet-up of a seasonally dry soil to understand the role of viruses in microbiome assembly. We found that dry soil is a low biomass yet highly rich seedbank of unique virions, and that resuscitation of the microbiome yields a bloom in biomass of a subset of viruses. Succession of the total pool of viruses is driven by spatial heterogeneity and nearly 50% of viral richness is lost in the first 24 hours following rewetting. We observed that, on a phylum level, active viral populations appear to follow temporal trends of their microbial hosts rather than serving as top-down controls. Further, contrary to the current paradigm, our data show that

lysogeny is not as prevalent in our system as previously hypothesized underscoring that the reservoir of soil viruses may be as virions rather than as inserts in microbial genomes. Our combined use of viromics, metagenomics, and isotopes facilitated estimation of the viral contribution to microbial mortality following rewetting. While our conservative calculations indicate viruses may not be the primary mechanism of observed mortality during microbiome assembly following rewetting, viruses appear to play an important and dynamic role in the microbial response following wet-up.

ACKNOWLEDGEMENTS

This research was supported by the U.S. Department of Energy (DOE) and Office of Biological and Environmental Research (BER) under awards DE-SC0020163 and DE-SC0016247 to M.K.F. Work conducted at Lawrence Livermore National Laboratory was supported by the U.S. DOE, BER, and Genomic Science Program Lawrence Livermore National Laboratory (LLNL) as part of 'Microbes Persist' Soil Microbiome Scientific Focus Area SCW1632 under the auspices of the U.S. DOE under contract DE-AC52-07NA27344. We acknowledge funding support to J.F.B. from the Chan Zuckerberg Biohub and the Innovative Genomics Institute at UC Berkeley.

We would like to thank Rachel Hestrin and Alexander Jaffe for helpful conversations regarding data analysis and visualization, and interpretations of isotopic data. We thank Katerina Estera-Molina for her expertise and management of the Firestone Lab field work site at the Hopland Research and Extension Center (HREC). Members of the Taga and Firestone labs provided helpful commentary and criticisms of this work. In particular, Maggie Yuan engaged in important conversations on statistical analyses. Rohan Sachdeva and Shufei Lei of the Banfield lab equipped this project with the necessary computational power and data management via the biotite server and ggKbase, respectively. Support staff at LLNL enabled the large-scale wet-up microcosm experiment and sample extractions, particularly Xiao Bin Max Li and Marissa Lafler.

We acknowledge that HREC sits on traditional, unceded land of the Pomo Indians. Research conducted at the University of California, Berkeley took place on the territory of xučyun (Huichin), the ancestral and unceded land of the Chochenyo-speaking Ohlone people, the successors of the sovereign Verona Band of Alameda County. This land was and continues to be of great importance to the Muwekma Ohlone Tribe and other familial descendants of the Verona Band.

J.F.B. is a founder of Metagenomi. The other authors declare no competing interests.

REFERENCES

1. Sokol NW, Slessarev E, Marschmann GL, Nicolas A, Blazewicz SJ, Brodie EL, et al. Life and death in the soil microbiome: how ecological processes influence biogeochemistry. *Nat Rev Microbiol* 2022; **0123456789**.
2. Yan Y, Klinkhamer PGL, van Veen JA, Kuramae EE. Environmental filtering: A case of bacterial community assembly in soil. *Soil Biol Biochem* 2019; **136**: 107531.
3. Romdhane S, Spor A, Aubert J, Bru D, Breuil MC, Hallin S, et al. Unraveling negative biotic interactions determining soil microbial community assembly and functioning. *ISME J* 2022; **16**: 296–306.
4. Zegeye EK, Brislawn CJ, Farris Y, Fansler SJ, Hofmockel KS, Jansson JK, et al. Selection, Succession, and Stabilization of Soil Microbial Consortia. *mSystems* 2019; **4**: 55–74.
5. Nemergut DR, Schmidt SK, Fukami T, O'Neill SP, Bilinski TM, Stanish LF, et al. Patterns

and Processes of Microbial Community Assembly. *Microbiol Mol Biol Rev* 2013; **77**: 342–356.
6. Wang C, Michalet R, Liu Z, Jiang X, Wang X, Zhang G, et al. Disentangling Large- and Small-Scale Abiotic and Biotic Factors Shaping Soil Microbial Communities in an Alpine Cushion Plant System. *Front Microbiol* 2020; **11**: 925.
7. Barnard RL, Blazewicz SJ, Firestone MK. Rewetting of soil: Revisiting the origin of soil CO2 emissions. *Soil Biol Biochem* 2020; **147**: 107819.
8. Blazewicz SJ, Hungate BA, Koch BJ, Nuccio EE, Morrissey E, Brodie EL, et al. Taxon-specific microbial growth and mortality patterns reveal distinct temporal population responses to rewetting in a California grassland soil. *ISME J* 2020; **14**: 1520–1532.
9. Placella SA, Firestone MK. Transcriptional response of nitrifying communities to wetting of dry soil. *Appl Environ Microbiol* 2013; **79**: 3294–302.
10. Williamson KE, Fuhrmann JJ, Wommack KE, Radosevich M. Viruses in Soil Ecosystems: An Unknown Quantity Within an Unexplored Territory. *Annu Rev Virol* 2017; **4**: 201–219.
11. Pratama AA, van Elsas JD. The 'Neglected' Soil Virome – Potential Role and Impact. *Trends Microbiol* 2018; **26**: 649–662.
12. Emerson JB. Soil Viruses: A New Hope. *mSystems* 2019; **4**: e00120-19.
13. Albright MBN, Gallegos-Graves LV, Feeser KL, Montoya K, Emerson JB, Shakya M, et al. Experimental evidence for the impact of soil viruses on carbon cycling during surface plant litter decomposition. *ISME Commun* 2022; **2**: 24.
14. Placella SA, Brodie EL, Firestone MK. Rainfall-induced carbon dioxide pulses result from sequential resuscitation of phylogenetically clustered microbial groups. *Proc Natl Acad Sci* 2012; **109**: 10931–10936.
15. Birch HF. The effect of soil drying on humus decomposition and nitrogen availability. *Plant Soil* 1958; **10**: 9–31.
16. Blazewicz SJ, Schwartz E, Firestone MK. Growth and death of bacteria and fungi underlie rainfall-induced carbon dioxide pulses from seasonally dried soil. *Ecology* 2014; **95**: 1162–1172.
17. Fraser FC, Corstanje R, Deeks LK, Harris JA, Pawlett M, Todman LC, et al. On the origin of carbon dioxide released from rewetted soils. *Soil Biol Biochem* 2016; **101**: 1–5.
18. Brum JR, Ignacio-Espinoza JC, Roux S, Doulcier G, Acinas SG, Alberti A, et al. Patterns and ecological drivers of ocean viral communities. *Science (80-)* 2015; **348**: 1261498.
19. Wilhelm SW, Suttle CA. Viruses and Nutrient Cycles in the Sea. *Bioscience* 1999; **49**: 781–788.
20. Suttle CA. Viruses in the sea. *Nature* . 2005. Nature Publishing Group. , **437**: 356–361
21. Roux S, Brum JR, Dutilh BE, Sunagawa S, Duhaime MB, Loy A, et al. Ecogenomics and potential biogeochemical impacts of globally abundant ocean viruses. *Nature* 2016; **537**: 689–693.
22. Weitz JS, Stock CA, Wilhelm SW, Bourouiba L, Coleman ML, Buchan A, et al. A multitrophic model to quantify the effects of marine viruses on microbial food webs and ecosystem processes. *ISME J* 2015; **9**: 1352–64.
23. Hurwitz BL, Hallam SJ, Sullivan MB. Metabolic reprogramming by viruses in the sunlit and dark ocean. *Genome Biol* 2013; **14**: R123.
24. Trubl G, Solonenko N, Chittick L, Solonenko SA, Rich VI, Sullivan MB. Optimization of viral resuspension methods for carbon-rich soils along a permafrost thaw gradient. *PeerJ* 2016; **4**: e1999.
25. Han L-L, Yu D-T, Zhang L-M, Shen J-P, He J-Z. Genetic and functional diversity of ubiquitous DNA viruses in selected Chinese agricultural soils. *Sci Rep* 2017; **7**: 45142.
26. Ackermann H-W. Sad State of Phage Electron Microscopy. Please Shoot the Messenger. *Microorganisms* 2013; **2**: 1–10.
27. Lennon JT, Jones SE. Microbial seed banks: the ecological and evolutionary implications

of dormancy. *Nat Rev Microbiol* 2011; **9**: 119–130.
28. Carini P, Marsden PJ, Leff JW, Morgan EE, Strickland MS, Fierer N. Relic DNA is abundant in soil and obscures estimates of soil microbial diversity. *Nat Microbiol* 2016; **2**: 16242.
29. Rousk J, Bååth E. Growth of saprotrophic fungi and bacteria in soil. *FEMS Microbiol Ecol* 2011; **78**: 17–30.
30. Couradeau E, Sasse J, Goudeau D, Nath N, Hazen TC, Bowen BP, et al. Probing the active fraction of soil microbiomes using BONCAT-FACS. *Nat Commun* 2019; **10**: 2770.
31. Pett-Ridge J, Firestone MK. Using stable isotopes to explore root-microbe-mineral interactions in soil. *Rhizosphere* 2017.
32. Radajewski S, Ineson P, Parekh NR, Murrell JC. Stable-isotope probing as a tool in microbial ecology. *Nature* 2000; **403**: 646–649.
33. Neufeld JD, Vohra J, Dumont MG, Lueders T, Manefield M, Friedrich MW, et al. DNA stable-isotope probing. *Nat Protoc* 2007; **2**: 860–866.
34. Schwartz E. Characterization of growing microorganisms in soil by stable isotope probing with H218O. *Appl Environ Microbiol* 2007; **73**: 2541–2546.
35. Hungate BA, Mau RL, Schwartz E, Caporaso JG, Dijkstra P, van Gestel N, et al. Quantitative microbial ecology through stable isotope probing. *Appl Environ Microbiol* 2015; **81**: 7570–81.
36. Koch BJ, McHugh TA, Hayer M, Schwartz E, Blazewicz SJ, Dijkstra P, et al. Estimating taxon-specific population dynamics in diverse microbial communities. *Ecosphere* 2018; **9**.
37. Greenlon A, Sieradzki ET, Zablocki O, Koch BJ, ... Quantitative stable-isotope probing (qSIP) with metagenomics links microbial physiology and activity to soil moisture in Mediterranean-climate grassland ecosystems. *bioRxiv* 2022.
38. Starr EP, Shi S, Blazewicz SJ, Koch BJ, Probst AJ, Hungate BA, et al. Stable-Isotope-Informed, Genome-Resolved Metagenomics Uncovers Potential Cross-Kingdom Interactions in Rhizosphere Soil. *mSphere* 2021; **6**.
39. Lee S, Sieradzki ET, Nicolas AM, Walker RL, Firestone MK, Hazard C, et al. Methane-derived carbon flows into host-virus networks at different trophic levels in soil. *Proc Natl Acad Sci U S A* 2021; **118**: 1–8.
40. Trubl G, Kimbrel JA, Liquet-Gonzalez J, Nuccio EE, Weber PK, Pett-Ridge J, et al. Active virus-host interactions at sub-freezing temperatures in Arctic peat soil. *Microbiome* 2021; **9**: 208.
41. Emerson JB, Roux S, Brum JR, Bolduc B, Woodcroft BJ, Jang H Bin, et al. Host-linked soil viral ecology along a permafrost thaw gradient. *Nat Microbiol* . 2018. , **3**: 870–880
42. Paez-Espino D, Eloe-Fadrosh EA, Pavlopoulos GA, Thomas AD, Huntemann M, Mikhailova N, et al. Uncovering Earth's virome. *Nature* 2016.
43. Reavy B, Swanson MM, Taliansky M. Viruses in Soil. 2014. pp 163–180.
44. Bi L, Yu D, Du S, Zhang L, Zhang L, Wu C, et al. Diversity and potential biogeochemical impacts of viruses in bulk and rhizosphere soils. *Environ Microbiol* 2020; **00**: 1462-2920.15010.
45. Williamson KE, Radosevich M, Smith DW, Wommack KE. Incidence of lysogeny within temperate and extreme soil environments. *Environ Microbiol* 2007; **9**: 2563–2574.
46. Ghosh D, Roy K, Williamson KE, White DC, Wommack KE, Sublette KL, et al. Prevalence of lysogeny among soil bacteria and presence of 16S rRNA and trzN genes in viral-community DNA. *Appl Environ Microbiol* 2008; **74**: 495–502.
47. Nafissi N, Slavcev R. Bacteriophage recombination systems and biotechnical applications. *Appl Microbiol Biotechnol* 2014; **98**: 2841–2851.
48. Correa AMS, Howard-Varona C, Coy SR, Buchan A, Sullivan MB, Weitz JS. Revisiting the rules of life for viruses of microorganisms. *Nat Rev Microbiol* 2021; **0123456789**.
49. Howard-Varona C, Hargreaves KR, Abedon ST, Sullivan MB. Lysogeny in nature:

mechanisms, impact and ecology of temperate phages. *ISME J* 2017; **11**: 1511–1520.
50. Ghosh D, Roy K, Williamson KE, Srinivasiah S, Wommack KE, Radosevich M. Acyl-homoserine lactones can induce virus production in lysogenic bacteria: An alternative paradigm for prophage induction. *Appl Environ Microbiol* 2009; **75**: 7142–7152.
51. Brum JR, Hurwitz BL, Schofield O, Ducklow HW, Sullivan MB. Seasonal time bombs: dominant temperate viruses affect Southern Ocean microbial dynamics. *ISME J* 2016; **10**: 437–49.
52. Jurgensen SK, Roux S, Schwenck SM, Stewart FJ, Sullivan MB, Brum JR. Viral community analysis in a marine oxygen minimum zone indicates increased potential for viral manipulation of microbial physiological state. *ISME J* 2022; **16**: 972–982.
53. Schimel JP. Life in dry soils: Effects of drought on soil microbial communities and processes. *Annu Rev Ecol Evol Syst* . 2018. Annual Reviews Inc. , **49**: 409–432
54. Kuzyakov Y, Mason-Jones K. Viruses in soil: Nano-scale undead drivers of microbial life, biogeochemical turnover and ecosystem functions. *Soil Biol Biochem* 2018; **127**: 305–317.
55. Knowles B, Silveira CB, Bailey BA, Barott K, Cantu VA, Cobian-Guëmes AG, et al. Lytic to temperate switching of viral communities. *Nature* 2016; **531**: 466–470.
56. Kimura M, Jia Z-J, Nakayama N, Asakawa S. Ecology of viruses in soils: Past, present and future perspectives. *Soil Sci Plant Nutr* 2008; **54**: 1–32.
57. Weitz JS, Beckett SJ, Brum JR, Cael BB, Dushoff J. Lysis, lysogeny and virus–microbe ratios. *Nature* 2017; **549**: E1–E3.
58. Wu R, Davison MR, Gao Y, Nicora CD, Mcdermott JE, Burnum-Johnson KE, et al. Moisture modulates soil reservoirs of active DNA and RNA viruses. *Commun Biol* 2021; **4**: 1–11.
59. Williamson KE, Radosevich M, Wommack KE. Abundance and diversity of viruses in six Delaware soils. *Appl Environ Microbiol* 2005; **71**: 3119–3125.
60. Barnard RL, Osborne CA, Firestone MK. Responses of soil bacterial and fungal communities to extreme desiccation and rewetting. *ISME J* 2013; **7**: 2229–2241.
61. McDaniel L, Paul JH. Effect of nutrient addition and environmental factors on prophage induction in natural populations of marine synechococcus species. *Appl Environ Microbiol* 2005; **71**: 842–50.
62. Williamson SJ, Houchin LA, McDaniel L, Paul JH. Seasonal Variation in Lysogeny as Depicted by Prophage Induction in Tampa Bay, Florida. *Appl Environ Microbiol* 2002; **68**: 4307–4314.
63. Sieradzki ET, Greenlon A, Nicolas AM, Firestone MK, Pett-Ridge J, Blazewicz SJ, et al. Functional succession of actively growing soil microorganisms during rewetting is shaped by precipitation history. *bioRxiv* 2022; 2022.06.28.498032.
64. Nicolas AM, Jaffe AL, Nuccio EE, Taga ME, Firestone MK, Banfield JF. Soil Candidate Phyla Radiation Bacteria Encode Components of Aerobic Metabolism and Co-occur with Nanoarchaea in the Rare Biosphere of Rhizosphere Grassland Communities. *mSystems* 2021; **6**.
65. Joshi N, Fass J. Sickle: A sliding-window, adaptive, quality-based trimming tool for FastQ files (Version 1.33). 2011.
66. Li D, Liu C-M, Luo R, Sadakane K, Lam T-W. MEGAHIT: an ultra-fast single-node solution for large and complex metagenomics assembly via succinct de Bruijn graph. *Bioinformatics* 2015; **31**: 1674–1676.
67. Hyatt D, Chen G-L, Locascio PF, Land ML, Larimer FW, Hauser LJ. Prodigal: prokaryotic gene recognition and translation initiation site identification. *BMC Bioinformatics* 2010; **11**: 119.
68. Edgar RC. Search and clustering orders of magnitude faster than BLAST. *Bioinformatics* 2010; **26**: 2460–2461.

69. Ogata H, Goto S, Sato K, Fujibuchi W, Bono H, Kanehisa M. KEGG: Kyoto encyclopedia of genes and genomes. *Nucleic Acids Res* . 1999. Oxford University Press. , **27**: 29–34
70. Suzek BE, Huang H, McGarvey P, Mazumder R, Wu CH. UniRef: comprehensive and non-redundant UniProt reference clusters. *Bioinformatics* 2007; **23**: 1282–1288.
71. Magrane M, Consortium U. UniProt Knowledgebase: a hub of integrated protein data. *Database* 2011; **2011**: bar009–bar009.
72. Wu Y-W, Tang Y-H, Tringe SG, Simmons BA, Singer SW. MaxBin: an automated binning method to recover individual genomes from metagenomes using an expectation-maximization algorithm. *Microbiome* 2014; **2**: 26.
73. Kang DD, Froula J, Egan R, Wang Z. MetaBAT, an efficient tool for accurately reconstructing single genomes from complex microbial communities. *PeerJ* 2015; **3**: e1165.
74. Alneberg J, Bjarnason BS, De Bruijn I, Schirmer M, Quick J, Ijaz UZ, et al. Binning metagenomic contigs by coverage and composition. *Nat Methods* 2014; **11**: 1144–1146.
75. Sieber CMK, Probst AJ, Sharrar A, Thomas BC, Hess M, Tringe SG, et al. Recovery of genomes from metagenomes via a dereplication, aggregation and scoring strategy. *Nat Microbiol* 2018; **3**: 836–843.
76. Olm MR, Brown CT, Brooks B, Banfield JF. dRep: a tool for fast and accurate genomic comparisons that enables improved genome recovery from metagenomes through de-replication. *ISME J* 2017; **11**: 2864–2868.
77. Roux S, Enault F, Hurwitz BL, Sullivan MB. VirSorter: mining viral signal from microbial genomic data. *PeerJ* 2015; **3**: e985.
78. Guo J, Bolduc B, Zayed AA, Varsani A, Dominguez-Huerta G, Delmont TO, et al. VirSorter2: a multi-classifier, expert-guided approach to detect diverse DNA and RNA viruses. *Microbiome* 2021; **9**: 37.
79. Kieft K, Zhou Z, Anantharaman K. VIBRANT: Automated recovery, annotation and curation of microbial viruses, and evaluation of viral community function from genomic sequences. *Microbiome* 2020; **8**: 90.
80. Jie Ren. Identifying viruses from metagenomic data by deep learning.
81. Auslander N, Gussow AB, Benler S, Wolf YI, Koonin E V. Seeker: Alignment-free identification of bacteriophage genomes by deep learning. *Nucleic Acids Res* 2020; **48**: E121.
82. Crits-Christoph A, Gelsinger DR, Ma B, Wierzchos J, Ravel J, Davila A, et al. Functional interactions of archaea, bacteria and viruses in a hypersaline endolithic community. *Environ Microbiol* 2016; **18**: 2064–2077.
83. Shaffer M, Borton MA, McGivern BB, Zayed AA, La Rosa SL 0003 3527 8101, Solden LM, et al. DRAM for distilling microbial metabolism to automate the curation of microbiome function. *Nucleic Acids Res* 2020; **48**: 8883–8900.
84. Barnard RL, Osborne CA, Firestone MK. Changing precipitation pattern alters soil microbial community response to wet-up under a Mediterranean-type climate. *ISME J* 2015; **9**: 946–957.
85. Uritskiy G V., Diruggiero J, Taylor J. MetaWRAP - A flexible pipeline for genome-resolved metagenomic data analysis 08 Information and Computing Sciences 0803 Computer Software 08 Information and Computing Sciences 0806 Information Systems. *Microbiome* 2018; **6**.
86. Chaumeil PA, Mussig AJ, Hugenholtz P, Parks DH. GTDB-Tk: A toolkit to classify genomes with the genome taxonomy database. *Bioinformatics* 2020; **36**: 1925–1927.
87. Li H, Handsaker B, Wysoker A, Fennell T, Ruan J, Homer N, et al. The Sequence Alignment/Map format and SAMtools. *Bioinformatics* 2009; **25**: 2078–2079.
88. Virtanen P, Gommers R, Oliphant TE, Haberland M, Reddy T, Cournapeau D, et al. SciPy 1.0: fundamental algorithms for scientific computing in Python. *Nat Methods* 2020;

17: 261–272.
89. Bland C, Ramsey TL, Sabree F, Lowe M, Brown K, Kyrpides NC, et al. CRISPR Recognition Tool (CRT): A tool for automatic detection of clustered regularly interspaced palindromic repeats. *BMC Bioinformatics* 2007; **8**: 209.
90. Altschul SF, Gish W, Miller W, Myers EW, Lipman DJ. Basic local alignment search tool. *J Mol Biol* 1990; **215**: 403–410.
91. Menzel P, Ng KL, Krogh A. Fast and sensitive taxonomic classification for metagenomics with Kaiju. *Nat Commun* 2016; **7**.
92. Shmakov SA, Sitnik V, Makarova KS, Wolf YI, Severinov K V, Koonin E V. The CRISPR Spacer Space Is Dominated by Sequences from Species-Specific Mobilomes. *MBio* 2017; **8**: e01397-17.
93. Al-Shayeb B, Sachdeva R, Chen LX, Ward F, Munk P, Devoto A, et al. Clades of huge phages from across Earth's ecosystems. *Nature* 2020; **578**: 425–431.
94. Mihara T, Nishimura Y, Shimizu Y, Nishiyama H, Yoshikawa G, Uehara H, et al. Linking Virus Genomes with Host Taxonomy. *Viruses* 2016; **8**: 66.
95. Kieft K, Anantharaman K. Deciphering Active Prophages from Metagenomes. *mSystems* 2022.
96. Waskom M. seaborn: statistical data visualization. *J Open Source Softw* 2021; **6**: 3021.
97. Klappenbach JA, Dunbar JM, Schmidt TM. rRNA operon copy number reflects ecological strategies of bacteria. *Appl Environ Microbiol* 2000; **66**: 1328–1333.
98. Williamson KE, Schnitker JB, Radosevich M, Smith DW, Wommack KE. Cultivation-based assessment of lysogeny among soil bacteria. *Microb Ecol* 2008; **56**: 437–47.
99. Sui B, Qi X, Wang X, Ren H, Liu W, Zhang C. Characterization of a Novel Bacteriophage swi2 Harboring Two Lysins Can Naturally Lyse Escherichia coli. *Front Microbiol* 2021; **12**: 1201.
100. Ignacio-Espinoza JC, Ahlgren NA, Fuhrman JA. Long-term stability and Red Queen-like strain dynamics in marine viruses. *Nat Microbiol* 2020; **5**: 265–271.
101. Nuccio EE, Blazewicz SJ, Lafler M, Campbell AN, Kakouridis A, Kimbrel JA, et al. HT-SIP: A semi-automated Stable Isotope Probing pipeline identifies interactions in the. *bioRxiv* 2022.
102. Roux S, Krupovic M, Daly RA, Borges AL, Nayfach S, Schulz F, et al. Cryptic inoviruses revealed as pervasive in bacteria and archaea across Earth's biomes. *Nat Microbiol* 2019; **4**: 1895–1906.
103. Chow C-ET, Kim DY, Sachdeva R, Caron DA, Fuhrman JA. Top-down controls on bacterial community structure: microbial network analysis of bacteria, T4-like viruses and protists. *ISME J* 2014; **8**: 816–829.
104. Van Goethem MW, Swenson TL, Trubl G, Roux S, Northen TR. Characteristics of Wetting-Induced Bacteriophage Blooms in Biological Soil Crust. *MBio* 2019; **10**.
105. Tecon R, Ebrahimi A, Kleyer H, Erev Levi S, Or D. Cell-to-cell bacterial interactions promoted by drier conditions on soil surfaces. *Proc Natl Acad Sci U S A* 2018; **115**: 9791–9796.
106. Jiao S, Yang Y, Xu Y, Zhang J, Lu Y. Balance between community assembly processes mediates species coexistence in agricultural soil microbiomes across eastern China. *ISME J* 2020; **14**: 202–216.
107. Santos-Medellín C, Estera-Molina K, Yuan M, Pett-Ridge J, Firestone MK, Emerson JB. Spatial turnover of soil viral populations and genotypes overlain by cohesive responses to moisture in grasslands. *bioRxiv* 2022.
108. Wilpiszeski RL, Aufrecht JA, Retterer ST, Sullivan MB, Graham DE, Pierce EM, et al. Soil Aggregate Microbial Communities: Towards Understanding Microbiome Interactions at Biologically Relevant Scales. *Appl Environ Microbiol* . 2019. NLM (Medline). , **85**
109. Jansson JK, Hofmockel KS. Soil microbiomes and climate change. *Nat Rev Microbiol* .

2020. Nature Research. , **18**: 35–46
110. Miller R V., Day MJ. Contribution of lysogeny, pseudolysogeny, and starvation to phage ecology. In: Abedon ST (ed). *Bacteriophage Ecology*. 2009. Cambridge University Press, Cambridge, pp 114–144.
111. Naylor D, Sadler N, Bhattacharjee A, Graham EB, Anderton CR, McClure R, et al. Soil microbiomes under climate change and implications for carbon cycling. *Annu Rev Environ Resour* . 2020. , **45**: 29–59
112. Jover LF, Effler TC, Buchan A, Wilhelm SW, Weitz JS. The elemental composition of virus particles: Implications for marine biogeochemical cycles. *Nat Rev Microbiol* 2014; **12**: 519–528.
113. Burstein D, Sun CL, Brown CT, Sharon I, Anantharaman K, Probst AJ, et al. Major bacterial lineages are essentially devoid of CRISPR-Cas viral defence systems. *Nat Commun* 2016; **7**: 10613.